

A THREE LAYER MODEL TO ESTIMATE PIT LAKE WATER QUALITY

A. Bermúdez¹, J.L. Delgado², L. M. García-García¹ and P. Quintela¹

¹*Dept. of Applied Mathematics, Universidade de Santiago de Compostela, 15782-Santiago, Spain*

²*Lignitos de Meirama, S.A.*

Abstract

By the end of 2007, “Lignitos de Meirama” open pit coal mine will cease its extraction activities definitively and a lake is expected to develop due to the hydrological conditions of the region. Its possible connection to a reservoir which supplies water to the city of A Coruña (NW Spain) enforces the mining company to fulfil the Spanish water quality standards. In this frame, prediction of the lake water quality at each stage of its flooding would constitute a very useful tool for the company in order to plan in advance any remediation action, in case it was required. This was the main goal of this work, which consisted of the development of a three-layer numerical model, each layer representing the lake surface, lake bottom and the rest of the water column respectively, to estimate the future lake water quality. Hydrological and geochemical processes were taken into account at each specific layer together with thermal phenomena, such as the surface heat transfer. The coupling of all these features allowed to the approximation of each layer density, therefore, the estimation of the periods in which a vertical stratification or vertical mixing was expected and the consequences on the lake water quality.

Introduction

Lignitos de Meirama open pit coal mine is located at the NW of Spain, approximately 25 km south of the city of A Coruña. More than 20 years of lignite extraction have left an open pit approximately 200 m deep, 1.5 km wide and 2.2 km long. Deep pits require continuous dewatering to avoid flooding as the mining operations proceed, being this practise especially important in this case due to the intense rainfall of the area. The deviation of a river that flew through Meirama valley by means of two channels that surround the mining zone was also needed to prevent water inflow into the pit.

When mining activities definitively stop, water pumping will cease and the deviated river water will be diverted into the pit. These entrances will constitute, together with the rain, the main water sources for the future pit lake.

Water quality of lakes generated at a former open pit mine present a wide variability, ranging from acidic, heavy metal-rich lakes (Berkeley pit, Montana), to near-neutral, low TDS ones (Cortez lake) (Miller et al., 1996). In general, chemical composition of a pit lake will depend on several factors that may change with time as it fills. Among these factors we highlight: 1) the chemical composition of the wall rocks, which is mainly related to the presence of iron sulfides at the pit walls and the environmentally hazardous consequences of their oxidation (heavy metal release and water acidification) and the possible existence of rock types with buffering capacity like carbonates or silicates; 2) the magnitude and geochemistry of the water sources flowing into the pit; 3) the precipitation/evaporation ratio; 4) the limnology of the future lake and its role in determining the transportation of chemical species through the water column; 5) the effect of biological activity (Miller et al., 1996; Castro et al., 2000; Davis, 2003; Howell, 2003).

In the case of “Lignitos de Meirama”, two rock types are exposed at the ultimate pit surface: granite and schists. Schists have a silicate composition with iron sulfides (pyrite, chalcopyrite) as main constituents. Sedimentary deposits as lignite and kaoliniferous shales are also present. Mine waste deposits with certain sulfide content fill partially the pit bottom and north wall. Sulfide oxidation of the mine waste deposits and the schist walls is evidenced by the chemical composition of the subterranean and infiltration water flowing through these lithologies (see Table 1). Although the magnitude of these sources is very small compared to the clean ones (basin/river water, rain and non-polluted subterranean waters), and they will only enter the pit for the first two years of flooding due to lake water level rise and the consequent decrease of the hydraulic gradient (according to the estimations of the mining company), they are highly polluted and may greatly affect the final water quality.

Table 1. Characteristics of the water sources into the pit (data in mg/L).

	pH	Fe	Al	Mn	SO ₄
Basin	7.06	0.1	1	0.04	4
Schist (clean)	6.61	2.5	1	1.08	106
Schist (polluted)	3.32	33	13.9	7.47	681
Granite (clean)	6.86	0.1	1	0.26	22
Granite (polluted)	7.07	0.38	1	0.72	149
Mine Wastes	3.01	38	11.5	16	986

It is evident that oxygen also plays an important role on the future lake water quality, that is the reason why predicting its limnological behaviour is so important. It is well known that natural lakes at warm latitudes usually exhibit seasonal patterns in which a spring-summer vertical stratification is followed by an autumn-winter vertical mixing. However, the behaviour of deep pit lakes is not necessarily the same, and the possibility of a complete vertical mixing will not only depend on the climate, but also on the dissolved solids concentration, the input from water sources and the pit lake morphology (Miller et al., 1996).

Notes on the future lake limnology

According to Hutchinson's definition of the lake "relative depth" (Z_r) (see Hutchinson, 1957) and his limnological classification of lakes based on this index (if $Z_r > 25\%$ the lake would be meromictic, otherwise holomictic), "Lignitos de Meirama" future pit lake ($Z_r = 13.4\%$ aprox.) should be holomictic, i.e. presenting vertical stratification in summer and complete turnover in winter. However, prediction of the future lake limnology cannot be based alone on this index as it demonstrates, for example, the case of Berkeley pit (Gammons et al., 2006), which is nowadays meromictic despite of its $Z_r = 20\%$, and other considerations regarding TDS and temperature have to be taken into account, as we have stated before.

A literature review on recent published geochemical and limnological considerations referred to existing pit lakes was very useful for us in order to understand and predict the most probable behaviour of our lake, always bearing in mind the specificities of each case. For example, a five years study on Lake St. Louis, France, a 60 m deep old open pit coal mine, has evidenced its meromictic nature, presenting a typical summer thermal stratification in three layers with winter turnover affecting only the upper, less dense layers and not the deeper monimolimnion, which is an "accumulation" of AMD affected waters, rich in TDS, that flow through mine waste deposits surrounding the mine pit and subterranean waters (see Denimal et al., 2005). Another five years study carried out on a shallower pit lake (24 m), the Summer Camp pit in Nevada, shows the different thermal and geochemical behaviour of the water column. Again, a three layer situation is described in summer, followed by winter vertical mixing that probably affected the whole water column except the last 1 m, due to the high density differences. This study constitutes as well an interesting example demonstrating how sporadic events, such as the collapse of a part of the pit wall, can eventually have an important influence on the water quality (Parshley et al., 2003).

Taking into account all the considerations above, we came to the conclusion that a typical stirred tank model could not faithfully reproduce the geochemistry of Lignitos de Meirama future pit lake. Instead, a three-layer model representing the lake surface, the lake bottom and the rest of the water column is proposed.

Methods/Governing Equations

Figure 1 illustrates the elements of our three-layer model. Figure 1A shows the adopted notation for each layer. In general, we will call $\Omega_\xi(t)$ the region of the space occupied by layer ξ ($\xi = 1,2,3$; with 1: surface layer, 2: bottom layer and 3: mid-depth layer) and $\Gamma^\xi(t) = \Gamma_S^\xi(t) \cup \Gamma_W^\xi(t) \cup \Gamma_M^\xi(t)$ its boundary, being $\Gamma_S^\xi(t)$, $\Gamma_W^\xi(t)$ and $\Gamma_M^\xi(t)$ the parts of the boundary of layer ξ representing the water/air interface, the water/pit wall interface and the interface between connected layers, respectively.

Surface layer $\Omega_1(t)$ will be characterized by a constant thickness of 10-15 m, which is approximately the thickness of the epilimnion during summer vertical stratification. The election of this layer will allow us simulating all the thermal phenomena that only take place at the air/water interface due to solar radiation effects, as well as site-specific geochemical phenomena, such as oxygen exchange with atmosphere. Bottom layer $\Omega_2(t)$ is formed by the accumulation of the subterranean and infiltration waters due to their higher densities in contrast to the less dense water that would form the upper layers (we recall that clean surface waters will be the main water entrance at our lake through the whole flooding period (see Table 1)). Finally, the mid-depth layer $\Omega_3(t)$ would represent the rest of the water column.

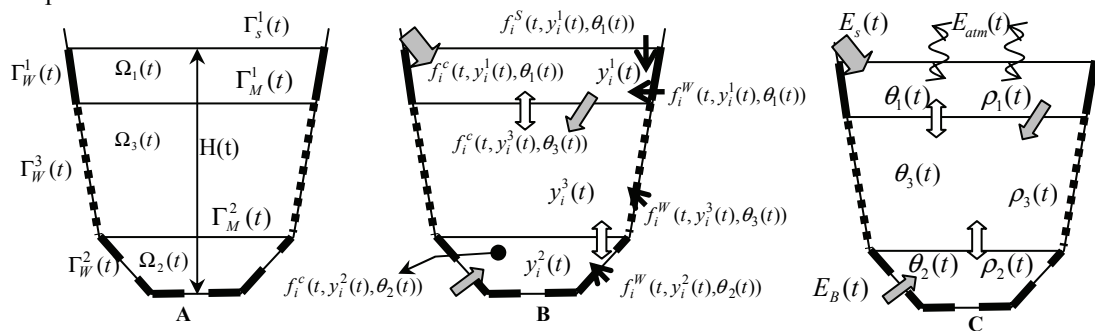


Figure 1. Three-layer model main elements; the symbols are described in the text.

Figure 1B depicts the main hydrogeochemical phenomena that will determine the future lake water quality. Let us call $y_i^\xi(t)$, the concentration of species i in the ξ -esim layer. The time evolution of this concentration will be represented by the following ordinary differential equation (ODE):

$$\begin{aligned} \frac{dy_i^\xi(t)}{dt} = & \frac{A(\Gamma_W^\xi(t))}{V_\xi(t)} f_i^W(t, Y^\xi(t), \theta_\xi(t)) + f_i^c(t, Y^\xi(t), \theta_\xi(t)) + \frac{A(\Gamma_S^\xi(t))}{V_\xi(t)} f_i^s(t, Y^\xi(t), \theta_\xi(t)) + \\ & \frac{1}{V_\xi(t)} \sum_{k=1}^{s(\xi)} q_{jk}(t) a_{i_{jk}}(t) - \frac{1}{V_\xi(t)} y_i^\xi(t) \frac{dV_\xi(t)}{dt} + G_i^\xi(t, d_i(\xi), c_i(\xi)), \end{aligned} \quad (1)$$

where $A(\Gamma_W^\xi(t))$ and $A(\Gamma_S^\xi(t))$ represent the areas of the water/pit wall and water/air interfaces, respectively; $V_\xi(t)$ is the volume of the ξ -th layer; $f_i^\zeta(t, Y^\xi(t), \theta_\xi(t))$ quantify the effect of the chemical reactions in which the i -th species is involved, denoting $\zeta = W$ the chemical reactions taking place at the pit wall/water interface (abiotic and biotic sulfide oxidation and silicate degradation), $\zeta = S$ the ones occurring at the water/air interface (oxygen reareation) and $\zeta = C$ the chemical reactions at the water column (abiotic and biotic ferrous iron oxidation, secondary minerals precipitation and heavy metal adsorption). The geochemical effect was calculated by assuming a kinetical approach, being the kinetical rate laws for the chemical reactions obtained from the literature (see García-García, 2005, for a more detailed description of the geochemical model). The fourth and fifth terms on the right hand side of eqn. (1) account for the effect of the water sources on the layer water quality (grey arrows in Fig.1B), with $q_{jk}(t)$ the magnitude of the sources entering layer ξ ($k = 1, \dots, s(\xi)$, being $s(\xi)$ the number of sources flowing into the layer) and $a_{i_{jk}}(t)$, the concentration of the i -th species on the k -th source. The last term stands for the effect on the i -th species of the concentration ($d_i(\xi)$) and density differences ($c_i(\xi)$) among layers in contact (white two-way arrows in Fig. 1B). For example, if we considered the surface layer, this term could be written as:

$$G_i^1(t, d_i(1), c_i(1)) = -(\alpha + \beta(\rho_1(t) - \rho_3(t))^+) (y_i^1(t) - y_i^3(t)), \quad (2)$$

being α and β the diffusion and convection coefficients respectively. $(\rho_1(t) - \rho_3(t))^+$ refers to the positive part of the difference inside, meaning that this term will only affect surface layer concentration when its density overcomes the one of the underlying layer.

The calculation of each layer density ($\rho_\xi(t)$), and hence stability of the water column, requires the consideration of the temperature ($\theta_\xi(t)$) effect. In this way, the three-layer model is completed by the thermal model represented in Figure 1C. For the sake of briefness, we will just show the time evolution of the temperature at the surface layer, because this is the only one directly affected by solar radiation (curly two-way arrows in Fig. 1C):

$$\begin{aligned} \frac{d\theta_1(t)}{dt} = & \frac{1}{\rho_1(t) C_e V_\xi} \left(A(\Gamma_S^1(t)) [Q_c(t) + \beta Q_{sw}(t) + Q_{lw} + Q_v] + \sum_{k=1}^{s(\xi)} \rho_{jk}(t) \theta_{jk}(t) C_e q_{jk}(t) - \right. \\ & \left. \rho_1(t) C_e \theta_1(t) \frac{dV_1(t)}{dt} - \rho_1(t) C_e \theta_1(t) \frac{dV_3(t)}{dt} \right) - (\alpha_\theta + \beta_\theta (\rho_1(t) - \rho_3(t))^+) (\theta_1(t) - \theta_3(t)), \end{aligned} \quad (3)$$

where the first term on the right accounts for the heat transfer with the atmosphere ($E_{atm}(t)$), with $Q_c(t)$ the heat flux due to convection, $Q_{sw}(t)$ the net flux due to short wave radiation, $Q_{lw}(t)$ the net flux due to long wave radiation and $Q_v(t)$ the heat loss due to evaporation. β represents the Lambert-Beer coefficient. C_e is the specific heat of water. The second and third terms describe the effect of the energy input due to the entrance of water sources into the pit ($E_s(t)$), being $\rho_{jk}(t)$ and $\theta_{jk}(t)$ the density and temperature of the k -th source. Fourth term refers to the energy transfer from the surface layer to the mid-depth layer due to the entrance of surface waters through the upper layer (grey arrow in between surface and mid-depth layer, Fig. 1C) and, finally, the last term comprises two effects: diffusion between layers due to temperature differences (α_θ is the diffusion coefficient) and convection due to density differences (β_θ is the convection coefficient).

Once the temperature and chemical composition of each layer is known, the density is approximated by using the following expression:

$$\rho_\xi(t) = \rho(\theta_\xi(t)) + \sum_{i=1}^N M_i y_i^\xi(t), \quad (4)$$

being $\rho(\theta_{\xi}(t))$ the part of the Unesco international equation of state for sea water regarding temperature dependence (Unesco, 1981) and M_i the molecular mass of the i -th species.

Results and Discussion

Results of the first stage of our work with the three-layer model in which α , β , α_0 and β_0 were equated to zero are shown in Figures 2 and 3. Figures 2A and 2B show the calculated layer temperature and density, respectively. As it can be seen, seasonal temperature oscillations are well reproduced at the surface layer, being attenuated at the mid-depth layer (water that forms this layer has previously flown through the surface layer). Temperature at the bottom remains constant at the whole simulation period, because the discharges and temperatures of the bottom sources are yearly constant. Calculated densities show the expected patterns according to temperature and dissolve solids content (see Fig. 2C to 2F). During the first winter, the water column is unstable, being the density of the surface higher than the mid-depth one and the latest higher than the bottom one. Under this situation, a complete vertical mixing would be expected. During summer, a complete vertical stratification would stabilize water column. However, next winter this stability will be broken, leading a vertical mixing affecting at least the first two layers. Figures 2C to 2F show some results on the future lake geochemistry. The pH of the surface and mid-depth layers (Fig. 2C) would be close to 5.5, being the one at the bottom around 3.5. The calculated heavy metal concentration (iron, aluminium and manganese) is in accordance to the obtained pH values, being their concentration much higher at the bottom than at the surface (Fig. 2D to 2F, respectively). These results agree with the observations made in similar lakes (see, for instance, Parshley et al., 2003; Denimal et al., 2005; Gammons et al., 2006). Although the effect of future lake limnology on the geochemistry is not included in these pictures, it can be inferred from the comments regarding water column stability we have just made. In this way, during first winter, the water quality of each layer should be very similar and equal to a mixture of all the layers.

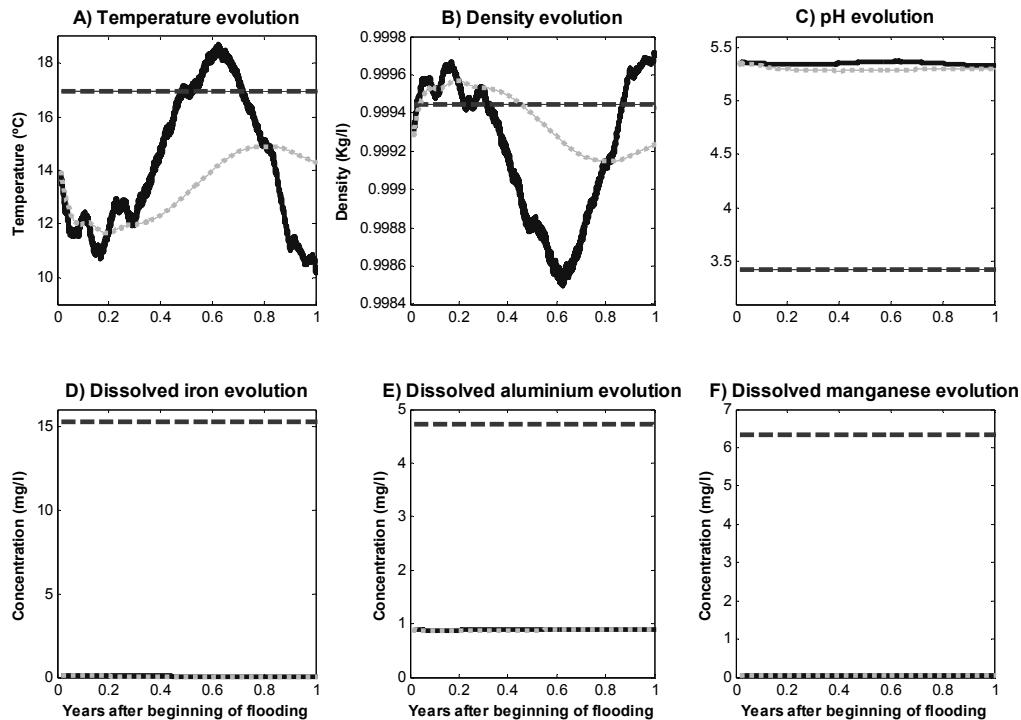


Figure 2. Three-layer model results. Full line: surface layer; dashed line: bottom layer; dotted line: mid-depth layer.

Going deeply into the future lake geochemistry, it is interesting for us to introduce a couple of comments on the surface pH. For this reason we show Figure 3, in which surface pH (A), dissolved aluminium (B) and dissolved iron (C) are represented. As we can see, pH values present seasonal oscillations which are proportional to the water temperature (these oscillations can be slightly observed in Fig. 2B). In fact, pH variability is related to aluminium hydroxide precipitation (we remind that hydroxide precipitation releases protons to the environment) which is higher in winter (due to the decrease of dissolved aluminium solubility with decreasing temperature,

Fig. 3B). The effect of ferric iron precipitation is also responsible for this pH value, but in a minor way (we can see that the entrance of aluminium through surface sources is high in comparison to iron entrances (Table 1), and higher than the ferric iron production due to pyrite oxidation). Finally, Figure 3C shows the dissolved iron concentration at the surface.

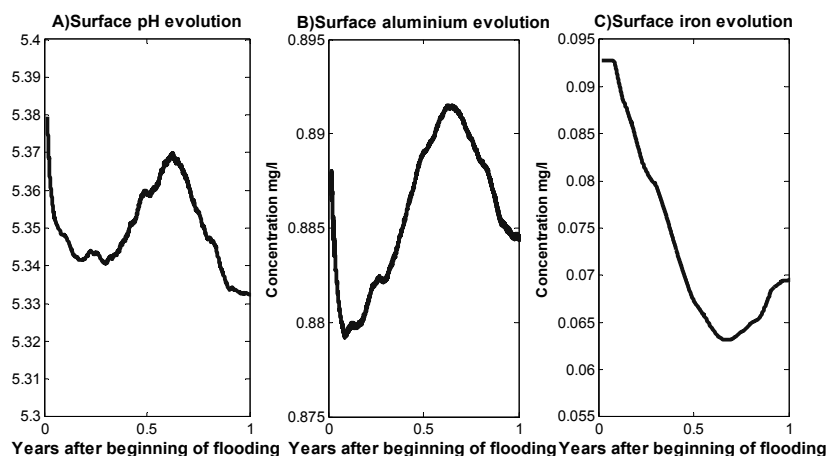


Figure 3. Some notes on surface geochemistry.

Conclusions

A three layer model resulted to be useful to estimate Lignitos de Meirama future pit lake water quality, even at a first stage in which α , β , α_0 and β_0 are considered zero. Results confirm that a complete vertical mixing will take place the first winter at least, with the consequent homogenisation of the water column from a geochemical point of view. In this way, a winter improvement on the bottom water quality is expected, in contrast to a slight deterioration on the surface one. During summer, the lake will be completely stratified, as it is usual in mid-latitude lakes. However, we are conscious of the fact that a faithful prediction of the water quality will require a proper consideration of diffusion and convection terms. A good estimation of these terms will let us know exactly the effect of vertical mixing on the variables of our model, such as the velocity of the chemical reactions (for example, we would be able to compute the effect of oxygen transfer to the generally anoxic bottom layer), etc. This is, therefore, the direction of our future work.

Acknowledgements

We greatly acknowledge Limeisa, S.A. for providing us the necessary data and support.

References

- Bowell R. (2003). Pit Lake Systematics: A Special Issue. *Mine Water and the Environment* 22, 167-169.
- Castro J.M., Moore J.N. (2000). Pit lakes: their characteristics and the potential for their remediation. *Environ. Geol.* 39, 1254-1260.
- Davis A. (2003). A Screening-Level Laboratory Method to Estimate Pit Lake Chemistry. *Mine Water and the Environment* 22, 194-205.
- Denimal S., Bertrand C., Mudry J., Paquette Y., Hochart M., Steinmann M. (2005). Evolution of the aqueous geochemistry of mine pit lakes-Blanzy-Montceau-les-Mines coal basin (Massif Central, France): origin of sulfate contents; effects of stratification on water quality. *Appl. Geochem.* 20, 825-839.
- Gammons C.H., Duime T.E. (2006). Long Term Changes in the Limnology and Geochemistry of the Berkeley Pit Lake, Butte, Montana. *Mine Water and the Environment* 25, 76-85.
- García-García L.M. (2005). Numerical simulation of the water quality of a lake. DEA Research work. Dpto. Matemática Aplicada. Universidad de Santiago de Compostela. (In Spanish).
- Hutchinson G.E. (1957). *A Treatise on Limnology. I. Geography, Physics, and Chemistry*, J. Wiley & Sons, New York, USA.
- Miller G.T., Lyons W.B., Davis A. (1996). Understanding the water quality of pit lakes. *Environ. Science and Technol.* 30, 118-123.
- Parshley J.V., Bowell R.J. (2003). The Limnology of Summer Camp Pit Lake: A Case Study. *Mine Water and the Environment* 22, 170-186.
- Unesco (1981). *The Practical Salinity Scale 1978 and the International Equation of State of Seawater 1980*. *Tech. Pap. Mar. Sci.* 36, 25 pp.